~~C-2~~

TECHNICAL REPORT
NATICK/TR-92/018

AD A245 054

STATIC ANALYSES OF ORTHOTROPIC AND NONLINEAR PRESSURE-LOADED MEMBRANES

By
John C. Brewer

December 1991

Final Report
October 1988 - September 1991

APPROVED FOR PUBLIC RELEASE;
DISTRIBUTION UNLIMITED

UNITED STATES ARMY NATICK
RESEARCH, DEVELOPMENT AND ENGINEERING CENTER
NATICK, MASSACHUSETTS 01760-5000

AERO-MECHANICAL ENGINEERING DIRECTORATE

U. S. ARMY NATICK RD&E CENTER
ATTN: STRNC-MIL
NATICK, MA 01760-5040

DISCLAIMERS

The findings contained in this report are not to be construed as an official Department of the Army position unless so designated by other authorized documents.

Citation of trade names in this report does not constitute an official endorsement or approval of the use of such items.

DESTRUCTION NOTICE

For Classified Documents:

Follow the procedures in DoD 5200.22-M, Industrial Security Manual, Section II-19 or DoD 5200.1-R, Information Security Program Regulation, Chapter IX.

For Unclassified/Limited Distribution Documents:

Destroy by any method that prevents disclosure of contents or reconstruction of the document.

REPORT DOCUMENTATION PAGE

Form Approved
OMB No. 0704-0188

Public reporting burden for this collection of information is estimated to average 1 hour per response, including the time for reviewing instructions, searching existing data sources, gathering and maintaining the data needed, and completing and reviewing the collection of information. Send comments regarding this burden estimate or any other aspect of this collection of information, including suggestions for reducing this burden, to Washington Headquarters Services, Directorate for Information Operations and Reports, 1215 Jefferson Davis Highway, Suite 1204, Arlington, VA 22202-4302, and to the Office of Management and Budget, Paperwork Reduction Project (0704-0188), Washington, DC 20503

1. AGENCY USE ONLY (Leave blank)	2. REPORT DATE	3. REPORT TYPE AND DATES COVERED
	December 1991	Final Oct. 1988-Sept. 1991

4. TITLE AND SUBTITLE

STATIC ANALYSES OF ORTHOTROPIC AND NONLINEAR PRESSURE-LOADED MEMBRANES

5. FUNDING NUMBERS

PE: 62786A
PR: 1L162786A427
WU: 1295003AA0E00
TA: A0
AG: T/B1292

6. AUTHOR(S)

John C. Brewer

7. PERFORMING ORGANIZATION NAME(S) AND ADDRESS(ES)

U.S. Army Natick Research, Development and Engineering Center
Kansas Street attn: STRNC-UE
Natick, MA-01760

8. PERFORMING ORGANIZATION REPORT NUMBER

NATICK/TR-92/018

9. SPONSORING/MONITORING AGENCY NAME(S) AND ADDRESS(ES)

10. SPONSORING/MONITORING AGENCY REPORT NUMBER

11. SUPPLEMENTARY NOTES

12a. DISTRIBUTION/AVAILABILITY STATEMENT

Approved for public release, distribution unlimited.

12b. DISTRIBUTION CODE

13. ABSTRACT (Maximum 200 words)

Analytical finite element studies were conducted for geometrically nonlinear pressure-loaded membranes. The membranes were composed of either orthotropic glass/epoxy composite materials or materially nonlinear (bilinear) aluminum. Three geometric configurations were studied: a rectangular membrane 40.5" (1029 mm) by 6.5" (165 mm), an "infinite" membrane 6.5" (165 mm) wide, and a square membrane 16.5" (419 mm) by 16.5" (419 mm). The NISA II finite element code was used for the analysis. Four node linear and eight node quadratic shell elements with six degrees of freedom per node were used. Quarter symmetry was assumed for the rectangular and square membranes. Half symmetry and appropriate side boundary conditions were used for the infinitely long membrane. The models employed simply supported boundary conditions at the membrane edges. Nonlinearities were treated by breaking the loading into small discrete steps. The geometry, stiffness matrix, and pressure loading were recomputed after each step. Elastically linear models exhibited cubic load-deflection behavior. That is, the pressure needed to produce a given deflection was proportional to the deflection cubed. The load-deflection behavior of the aluminum model was cubic until yielding and nearly linear thereafter. The ultimate strength of each glass/epoxy membrane was determined using the Tsai-Wu failure criterion. Results imply that composite fabric plies with the fibers oriented in the (Continued)

14. SUBJECT TERMS

MEMBRANES, GLASS/EPOXY, PRESSURE LOADING, FINITE ELEMENTS, STATIC ANALYSES, COMPOSITE MATERIALS, ORTHOTROPIC MATERIALS, NONLINEAR, TACTICAL SHELTERS

15. NUMBER OF PAGES

42

16. PRICE CODE

17. SECURITY CLASSIFICATION OF REPORT	18. SECURITY CLASSIFICATION OF THIS PAGE	19. SECURITY CLASSIFICATION OF ABSTRACT	20. LIMITATION OF ABSTRACT
UNCLASSIFIED	UNCLASSIFIED	UNCLASSIFIED	

Box 13. ABSTRACT (Continued):

principal directions of the membrane are the most efficient. The bilinear aluminum model indicates that metal membranes are promising, but post-yielding behavior should be investigated experimentally. Results also suggest that high aspect ratio membranes are more weight efficient. Analyses were conducted of infinitely long membranes with "hat" stiffeners. The stiffeners significantly affect the load-deflection behavior.

CONTENTS

	Page
List of Figures	v
List of Tables	vii
Preface	ix
Summary	1
Introduction	1
Finite Element Model	2
Results	7
Discussion	28
Conclusions	31
References	32
Appendix	33

DTIC COPY INSPECTED

Accession For
NTIS GRA&I ☑
DTIC TAB ☐
Unannounced ☐
Justification

By
Distribution/
Availability Codes
Dist | Avail and/or Special
A-1

LIST OF FIGURES

Figure		Page
1	Geometric Nonlinearity	3
2	Node and Element Locations for Rectangular Membranes	5
3	Infinite Membrane Model with Stiffener	8
4	Typical Pressure VS. Deflection Behavior	9
5	Deflection for A {0/90}s Glass/Epoxy Fabric Membrane	10
6	Pressure VS Deflection for a Bilinear Aluminum Membrane	11
7	Rectangular Composite Membrane-σxx Results at 25 psi	15
8	Rectangular Composite Membrane-σyy Results at 25 psi	16
9	Rectangular Composite Membrane-σxy Results at 25 psi	17
10	Square Composite Membranes-σxx Results at 25 psi	18
11	Composite Membrane-σyy Results at 25 psi	19
12	Composite Membrane-σxy Results at 25 psi	20
13	Infinite Composite Membrane-σxx Results at 25 psi	21
14	Infinite Composite Membrane-σyy Results at 25 psi	22
15	Rectangular Aluminum Membrane-Von Mises Stress Results (One Load Increment After Onset of Yielding)	23
16	Square Aluminum Membrane-Von Mises Stress Results (One Load Increment After Onset of Yielding)	24
17	Infinite Aluminum Membrane-Von Mises Stress Results (One Load Increment After Onset of Yielding)	25
18	Infinite Composite Membrane with Stiffener σxx Results at 25 psi	26
19	Infinite Composite Membrane with Stiffener σyy Results at 25 psi	27

LIST OF TABLES

Table		Page
1	Membrane Material Properties	6
2	Maximum Deflections of Glass/Epoxy Membranes at a pressure of 25 psi	12
3	Maximum Deflections of Bilinear Aluminum Membranes at 101.2 psi	13
4	Safety Factors for Glass/Epoxy Membranes at a Pressure of 25 psi	29

PREFACE

This research on static analyses of orthotropic and nonlinear pressure-loaded membranes was undertaken in the Engineering Technology Division of the Aero-Mechanican Engineering Directorate at the U.S. Army Natick Research, Development, and Engineering Center during the period October 1988 to September 1991. The funding was Program Element 62786A, Project 1L162786A427, Work Unit 1295003AA0E00, and Task A0.

STATIC ANALYSES OF ORTHOTROPIC AND NONLINEAR PRESSURE-LOADED MEMBRANES

Summary

Analytical finite element studies were conducted for geometrically nonlinear pressure-loaded membranes. The membranes were composed of either orthotropic glass/epoxy composite materials or materially nonlinear (bilinear) aluminum. Three geometric configurations were studied: a rectangular membrane 40.5" (1029 mm) by 6.5" (165 mm), an "infinite" membrane 6.5" (165 mm) wide, and a square membrane 16.5" (419 mm) by 16.5" (419 mm). The NISA II finite element code was used for the analysis. Four node linear and eight node quadratic shell elements with six degrees of freedom per node were used. Quarter symmetry was assumed for the rectangular and square membranes. Half symmetry and appropriate side boundary conditions were used for the infinitely long membrane. The models employed simply supported boundary conditions at the membrane edges. Nonlinearities were treated by breaking the loading into small discrete steps. The geometry, stiffness matrix, and pressure loading were recomputed after each step. Elastically linear models exhibited cubic load-deflection behavior. That is, the pressure needed to produce a given deflection was proportional to the deflection cubed. The load-deflection behavior of the aluminum model was cubic until yielding and nearly linear thereafter. The ultimate strength of each glass/epoxy membrane was determined using the Tsai-Wu failure criterion. Results imply that composite fabric plies with the fibers oriented in the principal directions of the membrane are the most efficient. The bilinear aluminum model indicates that metal membranes are promising, but post-yielding behavior should be investigated experimentally. Results also suggest that high aspect ratio membranes are more weight efficient. Analyses were conducted of infinitely long membranes with "hat" stiffeners. The stiffeners significantly affect the load-deflection behavior.

Introduction

Tactical shelters must be lightweight but also able to withstand dynamic overpressure loading. A prototype shelter employing a stiffened membrane construction has been shown effective in withstanding a blast wave. Design tools are needed to improve the weight efficiency of future membrane designs.

Membranes are extremely thin plates and by definition have negligible bending stiffness. As the center deflection of a pressure-loaded plate exceeds its thickness, membrane behavior begins to become important. Cylindrical bending analyses[1,2] are no longer valid as unreasonable deflections would be calculated for moderate values of pressure.

In membranes, stress is assumed constant through the thickness. Bending moments are counteracted by force components resulting from geometric nonlinearities as illustrated in Figure 1. Deflection is no longer proportional to applied pressure. Since undeflected membrane cannot have out-of-plane force components, the equations are singular at zero deflection and must be solved with numerical methods[3]. Specific isotropic cases, such as square and circular membranes[4] and membrane strips[5], have been solved numerically to show that deflection is proportional to the cube root of applied pressure and stress is proportional to pressure to the ⅔ power. This behavior results because the change in length of a ligament of the membrane for a given change in center deflection can be shown to be dominated by a term quadratic in out-of-plane deflection. Thus, strain (and therefore stress) levels are proportional to the square of the deflection.

A thermodynamic argument can then be used to understand the cubic behavior. Internal energy (strain energy) is proportional to the square of the strain level and thus deflection to the fourth power. The change in internal energy must be equal to the work done on the system, which takes the form of an integral of the pressure with respect to deflection. In order for such an integral to be proportional to deflection to the fourth power, the pressure must be proportional to the deflection cubed.

Dynamic analysis of a membrane struck by a pressure wave must consider that the membrane will react as a mass on a cubic spring rather than a linear spring. The dynamic magnification factor for a static equivalent load will not be two as is customary for linear systems. An analysis detailed in the Appendix shows that the static pressure that is needed to generate the displacement and stress states experienced at maximum deflection should be four times the dynamically applied value. Godfrey verified this with an isotropic membrane using a dynamic finite element analysis[6], although the deflection mode shape varied slightly from the static case. This discrepancy may result from the inability of the dynamic finite element code he used to account for the effect of changes in element size and orientation on the magnitude and direction of the pressure load after each time step.

Finite Element Model

Analytical finite element studies were conducted for geometrically nonlinear pressure-loaded membranes. The membranes were composed of either orthotropic glass/epoxy composite materials

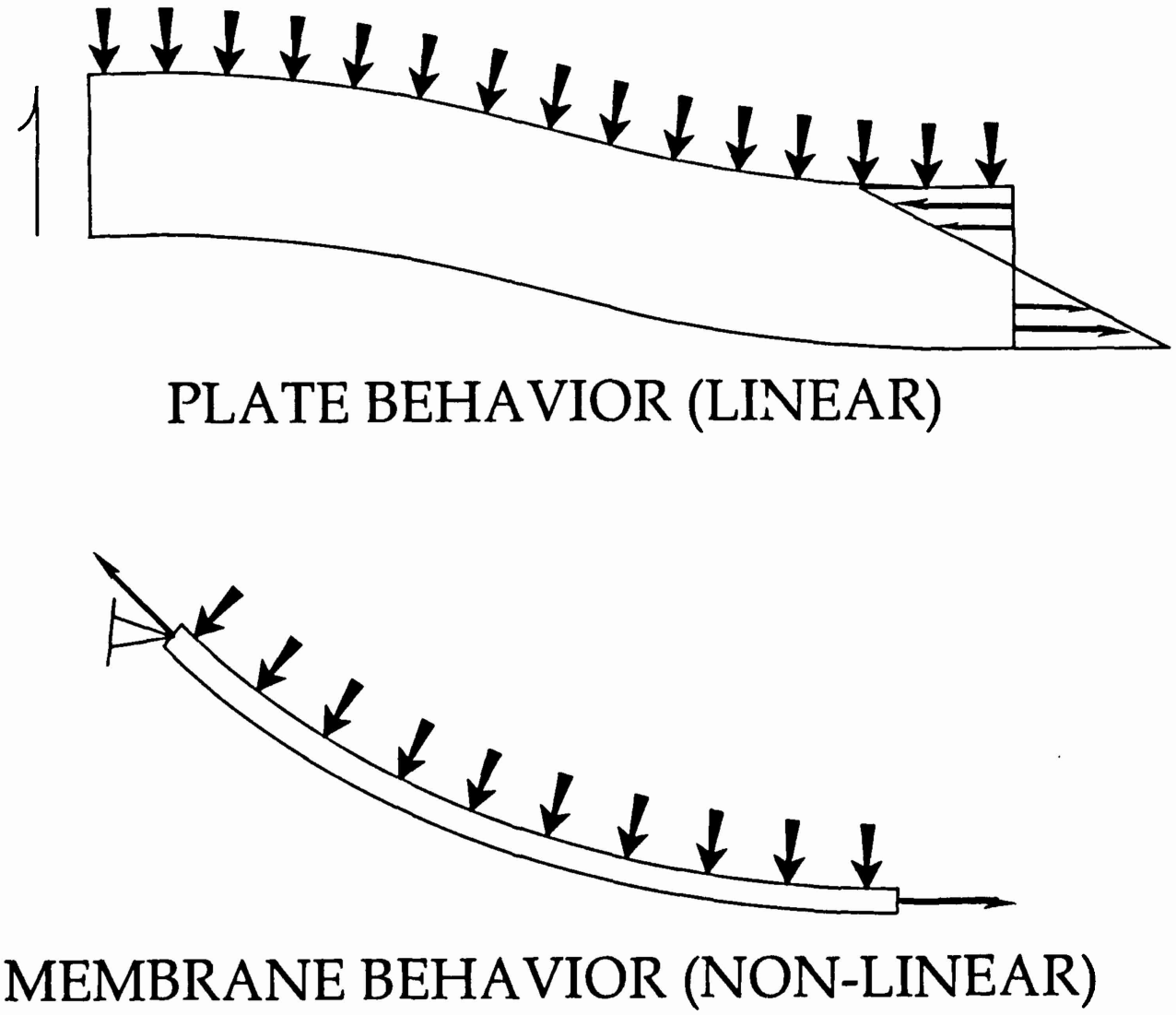

Figure 1: Geometric Nonlinearity

or materially nonlinear (bilinear) aluminum. Three geometric configurations were studied: a rectangular membrane 40.5" (1029 mm) by 6.5" (165 mm), an "infinite" membrane 6.5" (165 mm) wide, and a square membrane 16.5" (419 mm) by 16.5" (419 mm).

The glass/epoxy lamination sequences included fabric plies oriented along the major axes, along the membrane diagonals, at 45° to the major axes, or at 45° to the membrane diagonal. For the rectangular membrane, the appropriate lamination sequences were $[0/90]_s$, $[\pm 9.1]_s$, $[\pm 45]_s$, and $[\pm 35.9]_s$, respectively. For the infinite and square membranes, the fiber orientations are limited to $[0/90]_s$ and $[\pm 45]_s$. Lamination sequences were repeated with the addition of a 90° ply of unidirectional glass/epoxy tape for stiffening in the transverse direction.

The membrane thicknesses were 0.0293" for glass/epoxy membranes and 0.191" for aluminum membranes. The aluminum thickness was chosen to have the same areal density as the composite for comparison purposes. The properties of each membrane are given in Table 1.

The NISA II finite element code was used for the analysis. The elements were rectangular general three-dimensional shell elements. Four node linear elements were used for the orthotropic glass/epoxy and eight node quadratic elements were used for the isotropic aluminum. Both elements had three translational and three rotational degrees of freedom per node. The same nodal spacing was used for both glass/epoxy and aluminum membranes, so the glass/epoxy membrane models had four times as many elements. The element and node arrangement for the two types of models are shown in Figure 2. All models used simply supported boundary conditions at the membrane edges. Quarter symmetry was assumed for the rectangular and square membrane. The infinitely long membrane was assumed to be symmetric about the mid-span. The degrees of freedom at all nodes at each spanwise location were constrained to have the same values. This enforced the "boundary condition" in an infinite membrane that no quantity is a function of longitudinal position. In addition, no longitudinal displacement was allowed at any node.

The geometric and material nonlinearities were treated by breaking the loading (pressure level) into small discrete steps. The geometry, stiffness matrix, and pressure forces were automatically recomputed by the NISA software after each step. The first few steps had small enough deflections that a linear plate bending analysis was adequate. Once the deflections became significant, the recomputation of parameters was necessary. The results at each step were checked for convergence of reaction forces, internal energy, and displacement. The selection of load increments for each analysis involved some trial and error. Small load increments yielded computationally intensive analyses while large increments hampered convergence. The composite membranes were loaded to a 25.0 psi applied pressure load. Since aluminum membranes can undergo yielding, their load-deflection behavior can change. They were analyzed to the static pressure that would

COMPOSITE

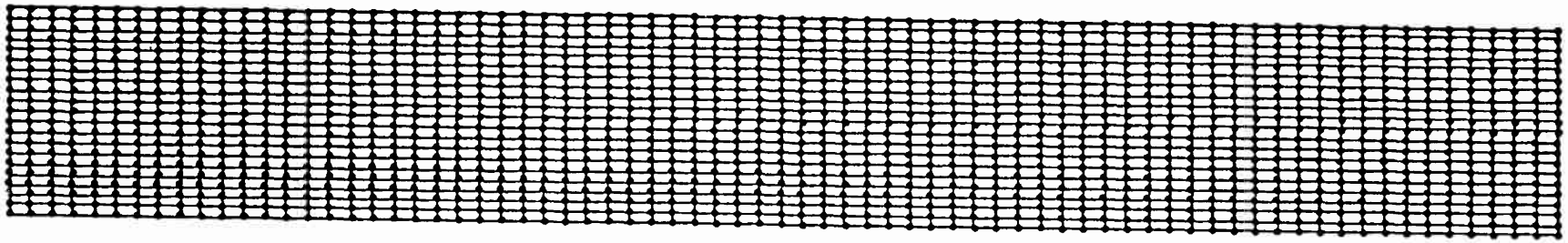

ALUMINUM

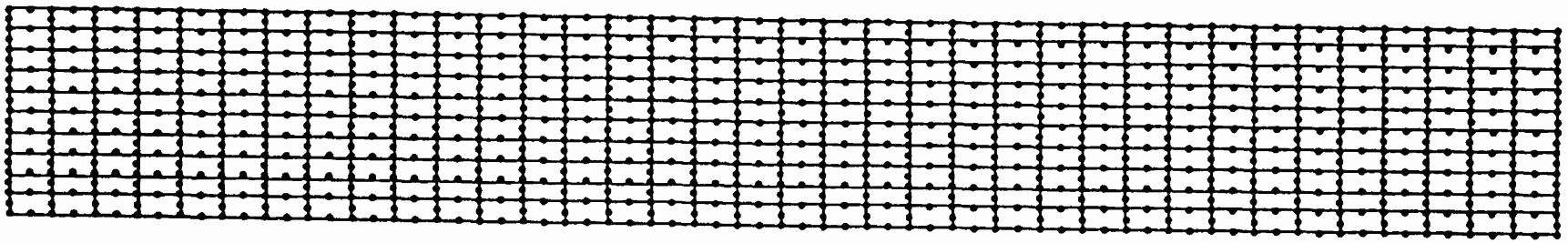

Figure 2: Node and Element Locations for Rectangular Membranes

Table 1: Membrane Material Properties

Lamination Sequence[a]	Longitudinal Modulus E_L [msi]	Transverse Modulus E_T [msi]	Shear Modulus G [msi]	Poisson's Ratio ν
$[0_f/90_f]_s$	3.40	3.40	1.00	0.10
$[0_f/90_f/\overline{90}_t]_s$	2.90	3.93	0.86	0.09
$[\pm 9.1_f]_s$	3.40	3.27	1.05	0.12
$[\pm 9.1_f/\overline{90}_t]_s$	2.91	3.83	0.90	0.10
$[\pm 35.9_f]_s$	2.73	2.69	1.49	0.29
$[\pm 35.9_f/\overline{90}_t]_s$	2.44	3.39	1.23	0.20
$[\pm 45_f]_s$	2.62	2.62	1.54	0.31
$[\pm 45_f/\overline{90}_t]_s$	2.37	3.34	1.27	0.21
Aluminum	E = 10.0 msi	ν = 0.33	σ_{yield} = 35 ksi	
	ϵ_{ult} = 12.0%	σ_{ult} = 42 ksi		

produce the equivalent deflection, stress, and strain distribution. When a 10 psi pressure wave strikes a flat surface, the effective pressure is enhanced by fluid dynamic reflection to a peak level of 25.3 psi. The duration at or near this peak exceeds the time needed for the membranes to respond. If the load-deflection behavior of the membrane remained cubic, the equivalent static pressure load would be four times the peak level, or 101.2 psi.

Analyses were conducted on infinite membranes with "hat" stiffeners. The stiffeners were 5.5" (140 mm) across and 2.86" (73 mm) high. The boundary condition was that the centerline of the stiffener was clamped at both its upper and lower surfaces and that the centerline of its lower surface was fixed. This model is illustrated in Figure 3.

Results

The center deflection was determined for each finite element model at each load increment. A typical load-deflection curve is shown in Figure 4. A linear regression was run on the logarithm of the load versus the logarithm of the deflection. The slope of the regression yields the order of the relationship (i.e., an exponent of one for a linear relationship, an exponent of three for a cubic relationship). The correlation coefficient, R, gives an indication of the quality of the fit of the regression, with a value of 1.0 indicating a perfectly straight line. Since the first load steps yield deflection on the order the membrane thickness, they are dominated by linear plate theory effects. Thus, only calculated deflections which exceeded five times the membrane thickness were included. The load-deflection behavior of the bilinear aluminum models changed after the onset of yielding, so points after the onset of yielding were not included.

Figure 5 shows a typical linear regression of calculated load and deflection values for a composite membrane. Figure 6 shows a typical linear regression of calculated load and deflection values for a bilinear aluminum membrane. The regressions for the membranes yielded exponent values between 2.995 and 3.002 with correlation coefficients ranging from 0.9999996 to 0.999999998, indicating nearly perfect cubic behavior. The regressions on the aluminum membranes after they had experienced yielding over the majority of their area produced exponents ranging from 1.060 to 1.069 with correlation coefficients from 0.99988 too 0.99992, indicating nearly linear behavior. Table 2 shows the center deflection of the composite membranes at 25 psi. Table 3 contains the maximum center deflections experienced by the aluminum membranes at 101.2 psi.

The models of infinite membranes with stiffeners at the membrane boundary did not display cubic load-deflection behavior. The exponents for the membranes ranged from 2.302 to 2.322 with correlation coefficients from 0.99990 to 0.99994. A regression was also run on the load data versus the difference in deflection from

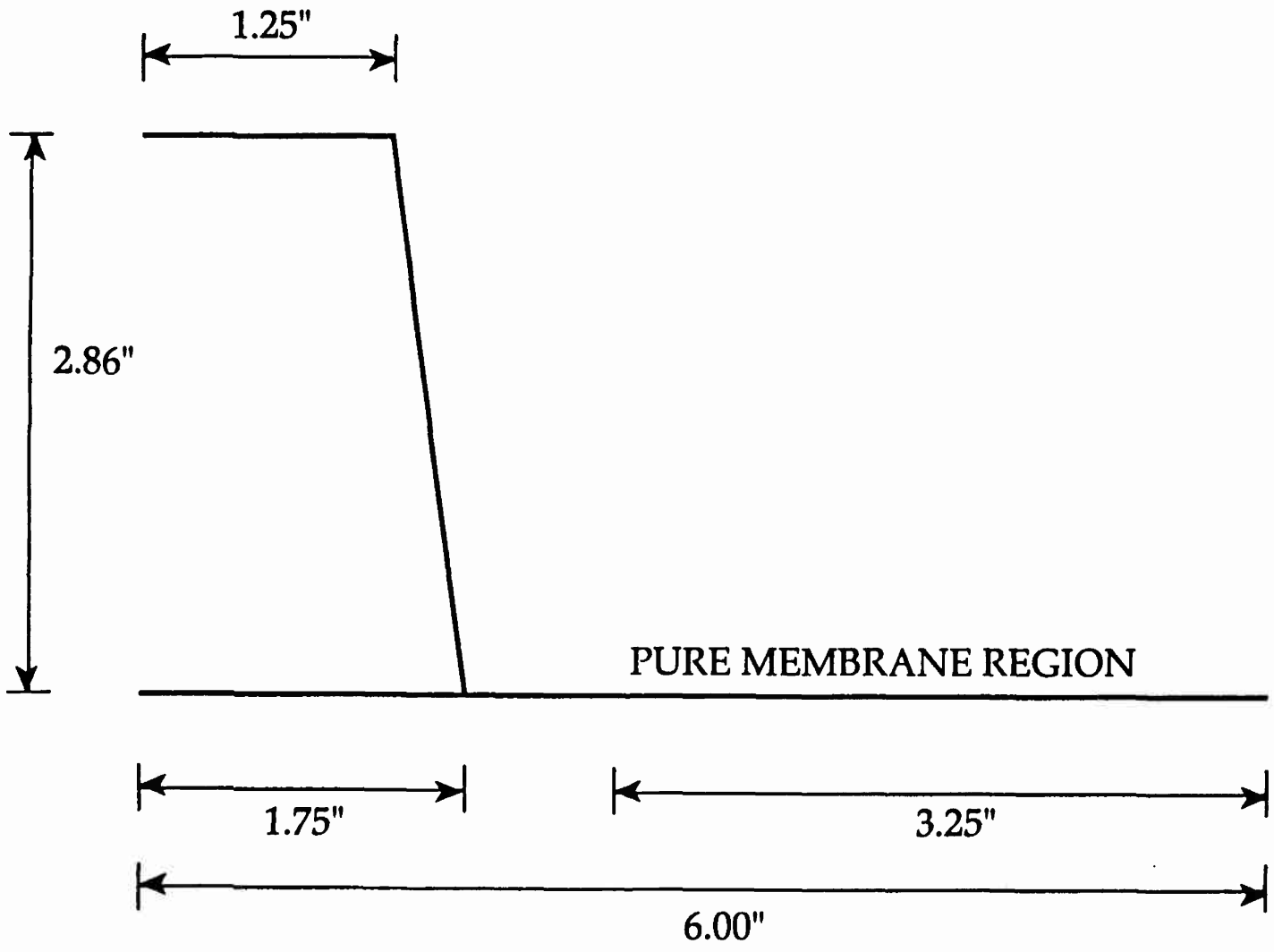

Figure 3: Infinite Membrane Model with Stiffener

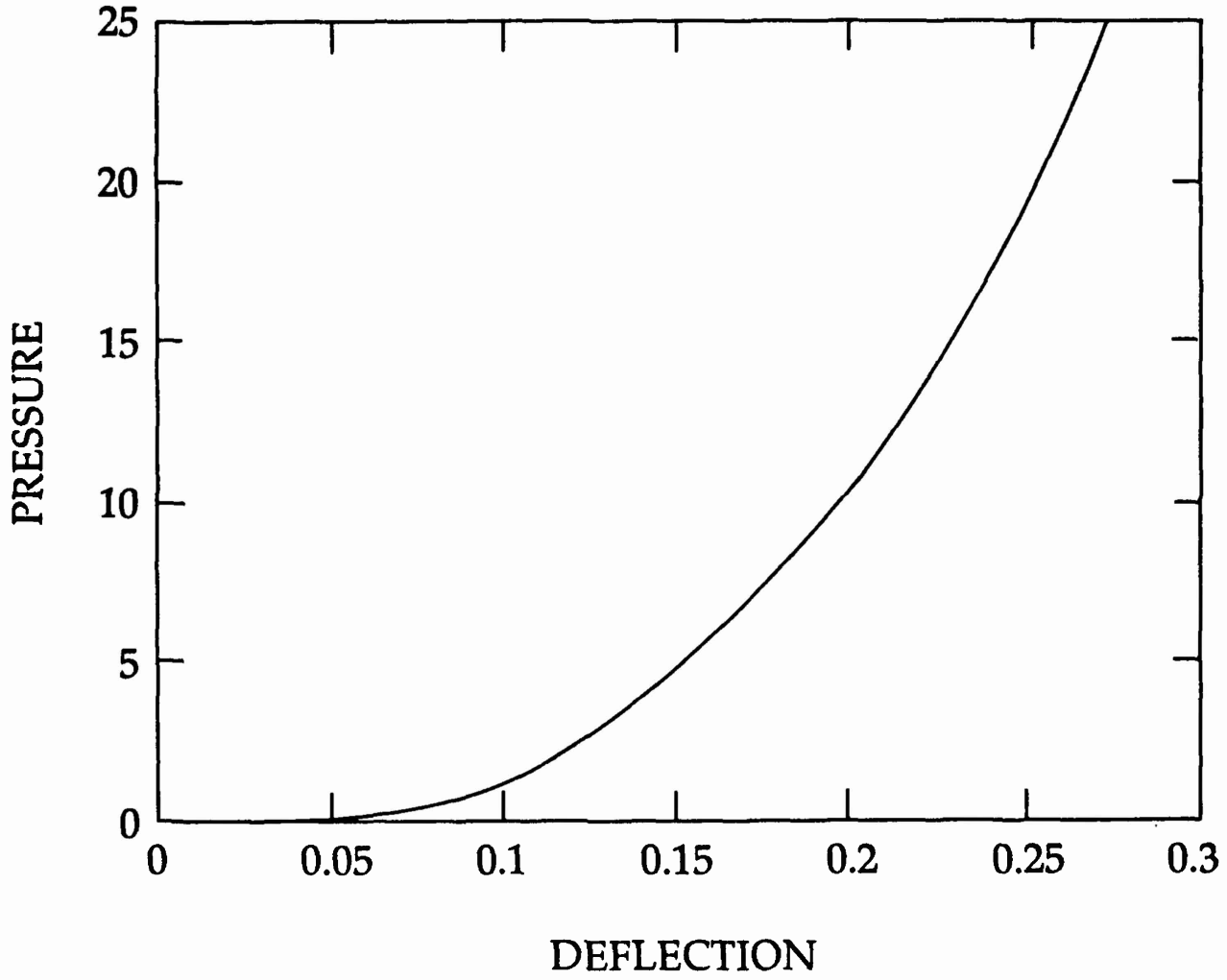

Figure 4: Typical Pressure VS. Deflection Behavior

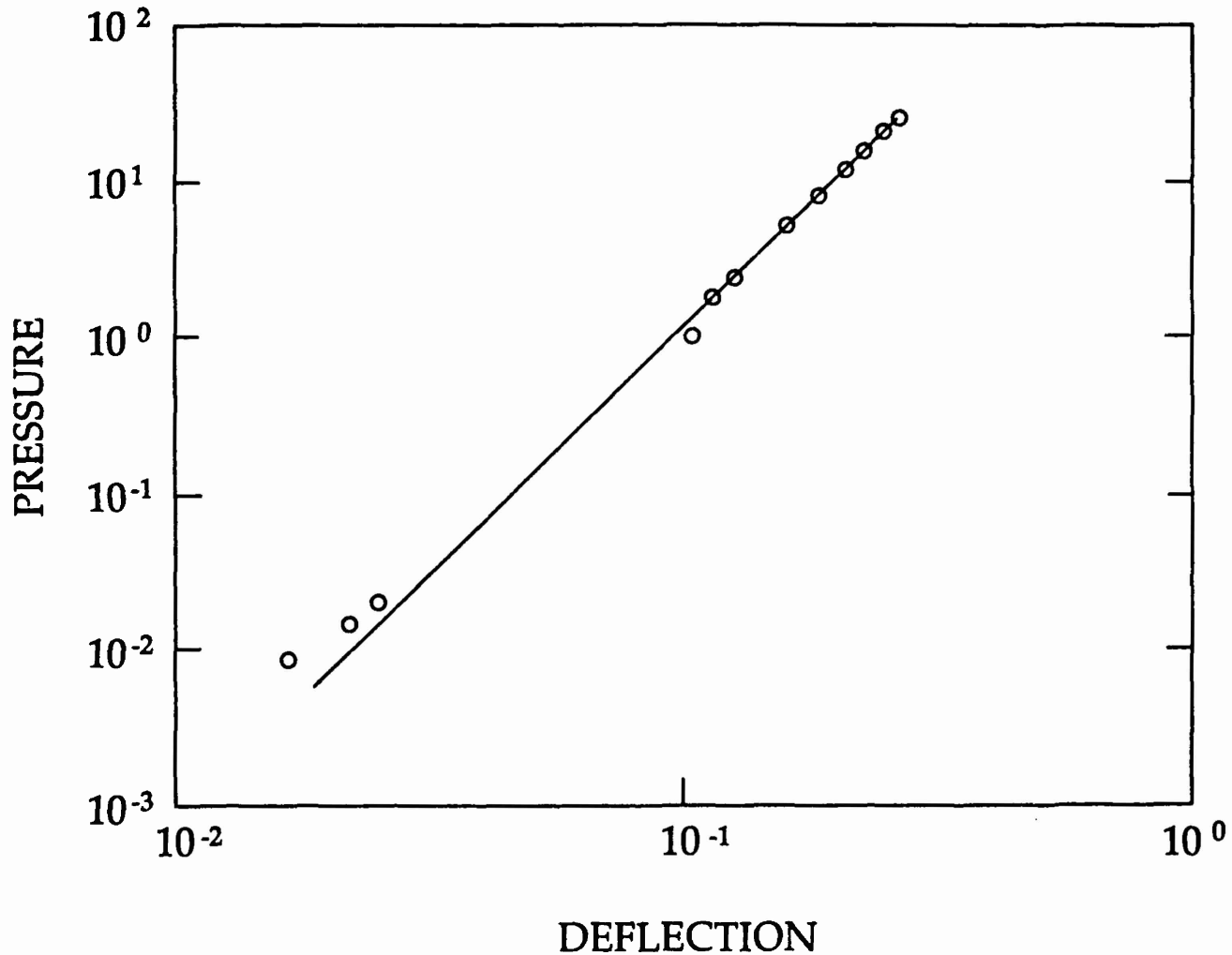

Figure 5: Deflection for A {0/90}s Glass/Epoxy Fabric Membrane

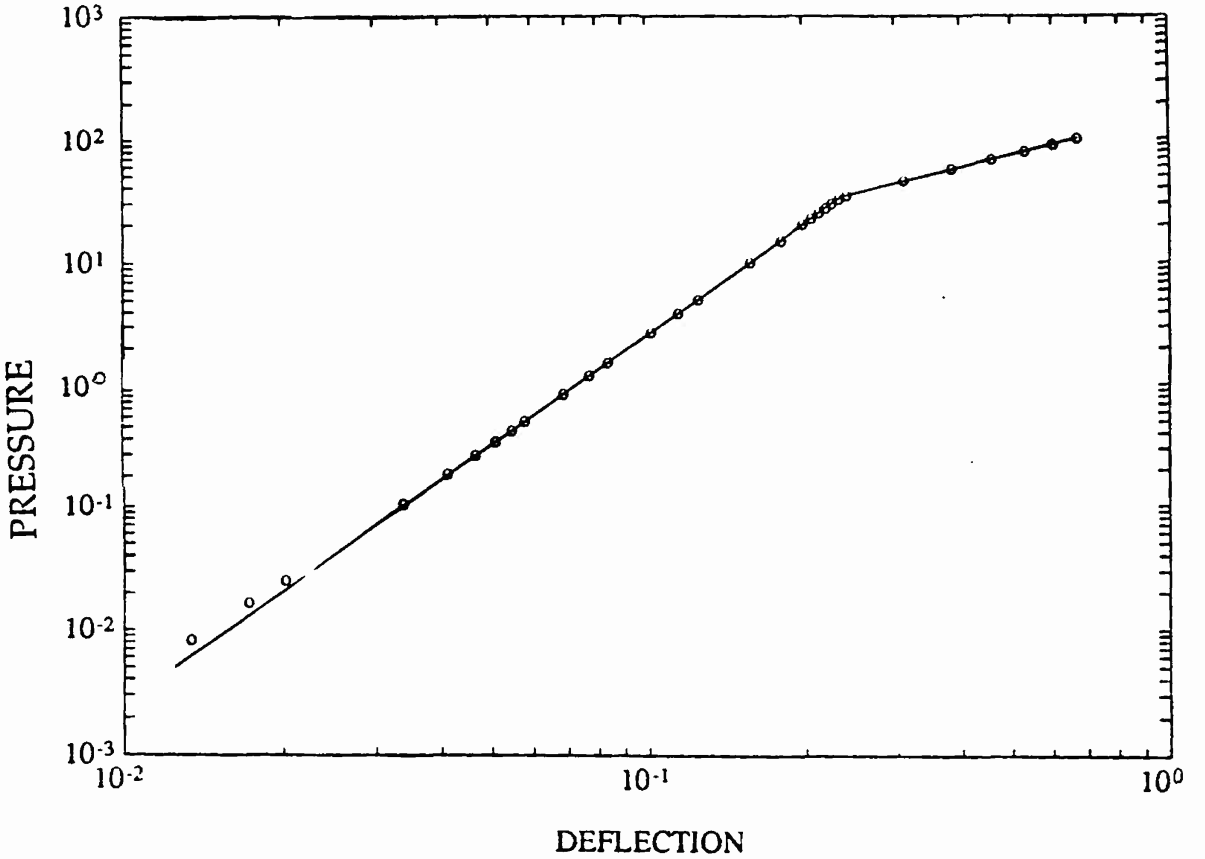

Figure 6: Pressure VS Deflection for a Bilinear Aluminum Membrane

Table 2: Maximum Deflections of Glass/Epoxy Membranes at a Pressure of 25 psi[a]

Lamination Sequence	Infinite Membrane	Rectangular Membrane	Square Membrane	Infinite Membrane with Stiffener
$[0_f/90_f]_s$	0.275	0.275	0.805	0.462
$[0_f/90_f/\overline{90}_t]_s$	0.262	0.262	0.802	0.443
$[\pm 9.1_f]_s$	—	0.278	—	—
$[\pm 9.1_f/\overline{90}_t]_s$	—	0.264	—	—
$[\pm 35.9_f]_s$	—	0.290	—	—
$[\pm 35.9_f/\overline{90}_t]_s$	—	0.271	—	—
$[\pm 45_f]_s$	0.291	0.291	0.832	0.488
$[\pm 45_f/\overline{90}_t]_s$	0.272	0.272	0.821	0.456

[a] Dimensions are inches

Table 3: Maximum Deflection of Bilinear Aluminum Membranes at 101.2 psi[a]

Infinite Membrane	0.668
Rectangular Membrane	0.668
Square Membrane	2.683
Infinite Membrane with Stiffener (Total Deflection)	0.633
Infinite Membrane with Stiffener (Relative to Membrane Edge)	0.243

[a] Dimensions are inches

the center of the membrane to the boundary between the membrane and the stiffener. In this case, the exponents ranged from 3.748 to 3.975 with correlation coefficients ranging from 0.99794 to 0.99840. After the aluminum membrane had experienced yielding, its exponent for center deflection was 2.608 with a correlation coefficient of 0.99994 and its exponent for the difference in deflections was 4.532 with a correlation coefficient of 0.99989.

The stress distribution was determined for each model at each load. Figures 7 through 12 show typical distributions of the in-plane stresses σ_{11}, σ_{22}, and σ_{12} for rectangular and square composite membranes at maximum pressure load of 25 psi. It can be seen that even with a 90° tape ply, the σ_{22} distribution for the square membrane is similar to a rotated version of the σ_{11} distribution. Figures 13 and 14 show typical distributions of σ_{11} and σ_{22} for infinite composite membranes at a 25 psi pressure load. The σ_{12} values are identically zero for this configuration. Figures 15 through 17 show distributions of von Mises equivalent stress for the rectangular, square, and infinite bilinear aluminum membrane models, respectively, at the first load increment after the onset of yielding. Figures 18 and 19 show typical distributions of σ_{11} and σ_{22} for infinite composite membranes with stiffeners at a 25 psi pressure load.

Safety factors were determined for each glass/epoxy membrane using the Tsai-Wu failure criterion. The stress state in each ply was calculated from the laminate stress level when the applied pressure was 25 psi. The failure criterion was then applied on a ply by ply basis. The safety factor for any point in the stress distribution is defined as the ratio of the stress state that would cause failure to the stress state calculated. The safety factor for the membrane is defined as the lowest safety factor of all points on the membrane. Two types of safety factors are listed for each composite membrane. The first ply failure (FPF) safety factor relates to that stress distribution which causes the first failure at any point in any ply. Failure of an individual ply need not imply failure of all plies at that location. The ultimate stress safety factor relates to that stress distribution which causes all plies at a given point to fail.

The calculation of ultimate failure at a point depends on assumptions made about ply properties and stress distribution after first ply failure occurs. In the analyses in this paper, there were two types of failure: the simultaneous failure of all plies (when all the plies were glass/epoxy fabric) and the failure of an individual 90° unidirectional glass/epoxy tape ply. The damage area after first ply failure was assumed to be small, so the laminate stress distribution was assumed not to change. That is, the total stress level remained the same, but there was some redistribution of load between plies. Since the 90° plies failed primarily in transverse tension, it was assumed that matrix properties (transverse strength and stiffness, shear strength and stiffness) but not fiber properties (longitudinal strength and stiffness) were lost. The stresses were recalculated for each ply in the damaged

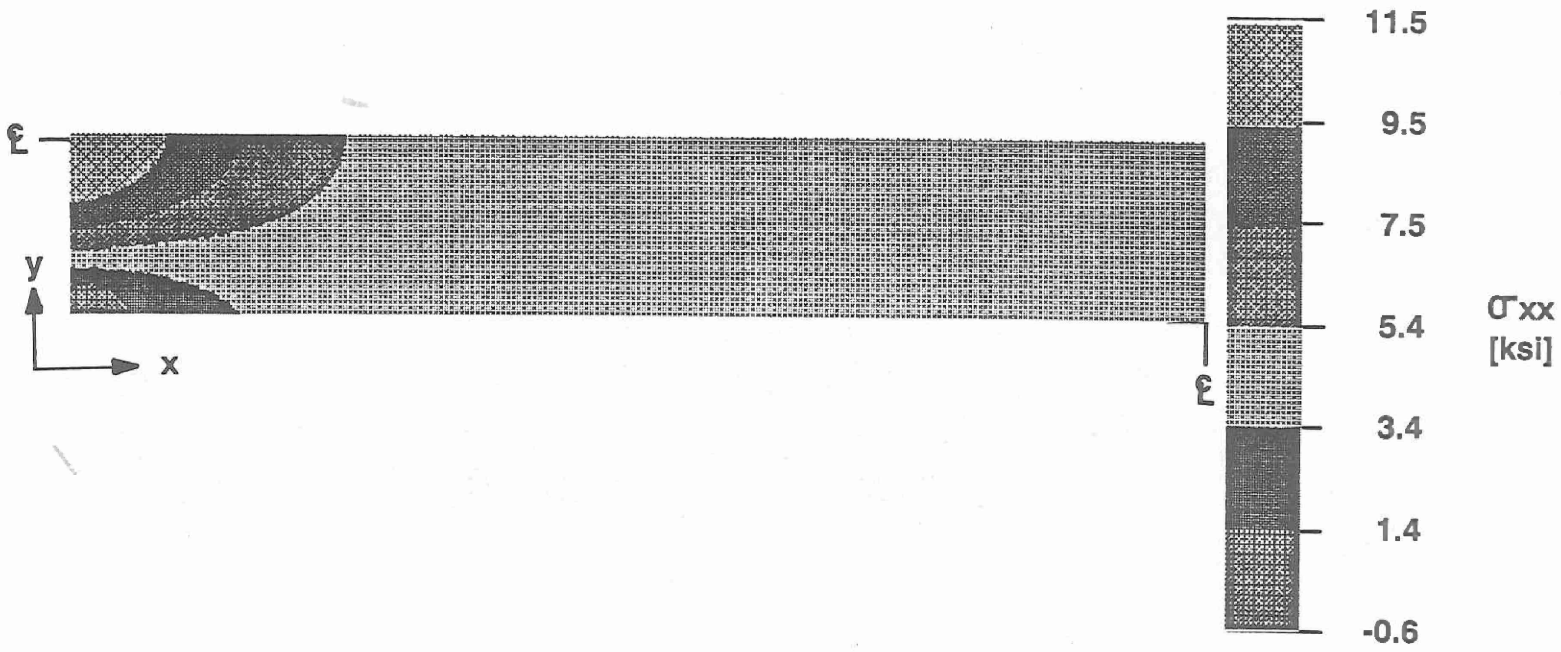

Figure 7: Rectangular Composite Membrane - σxx Results at 25 PSI

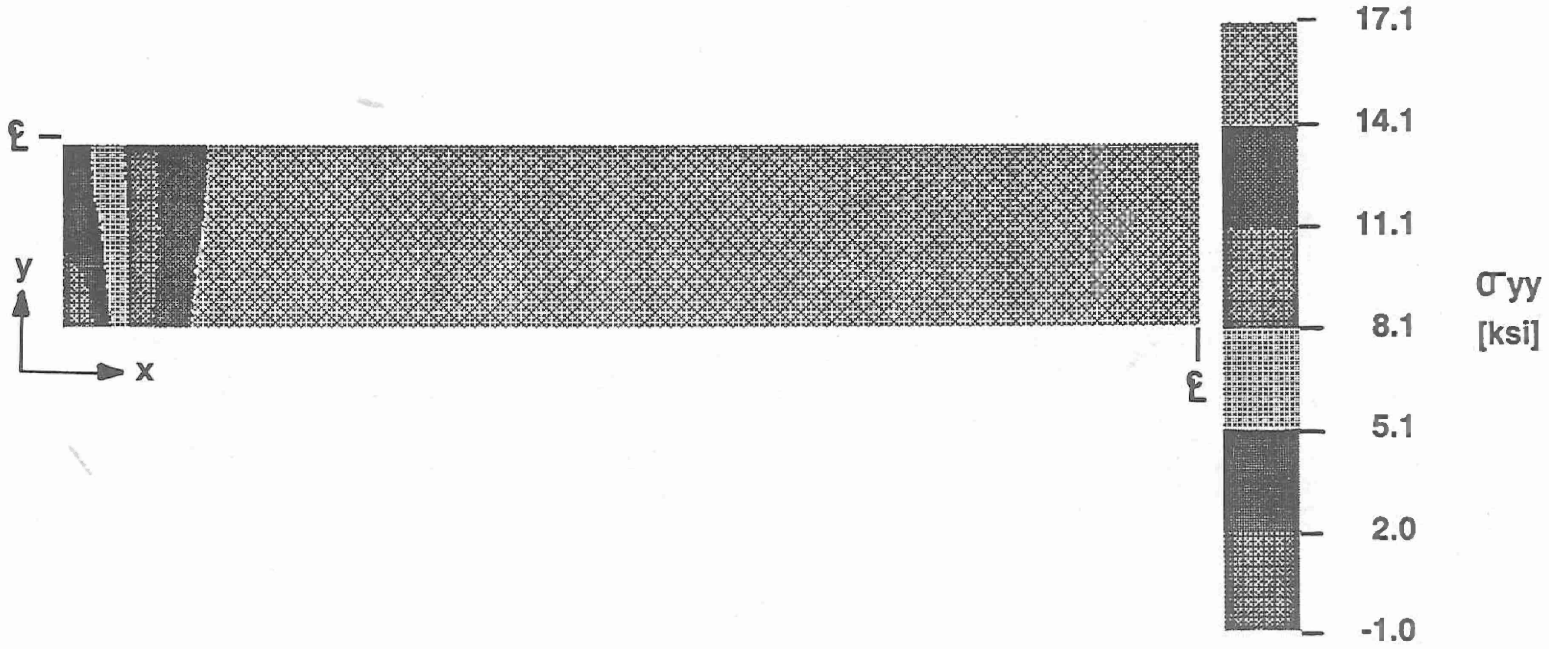

Figure 8: Rectangular Composite Membrane - σyy Results at 25 PSI

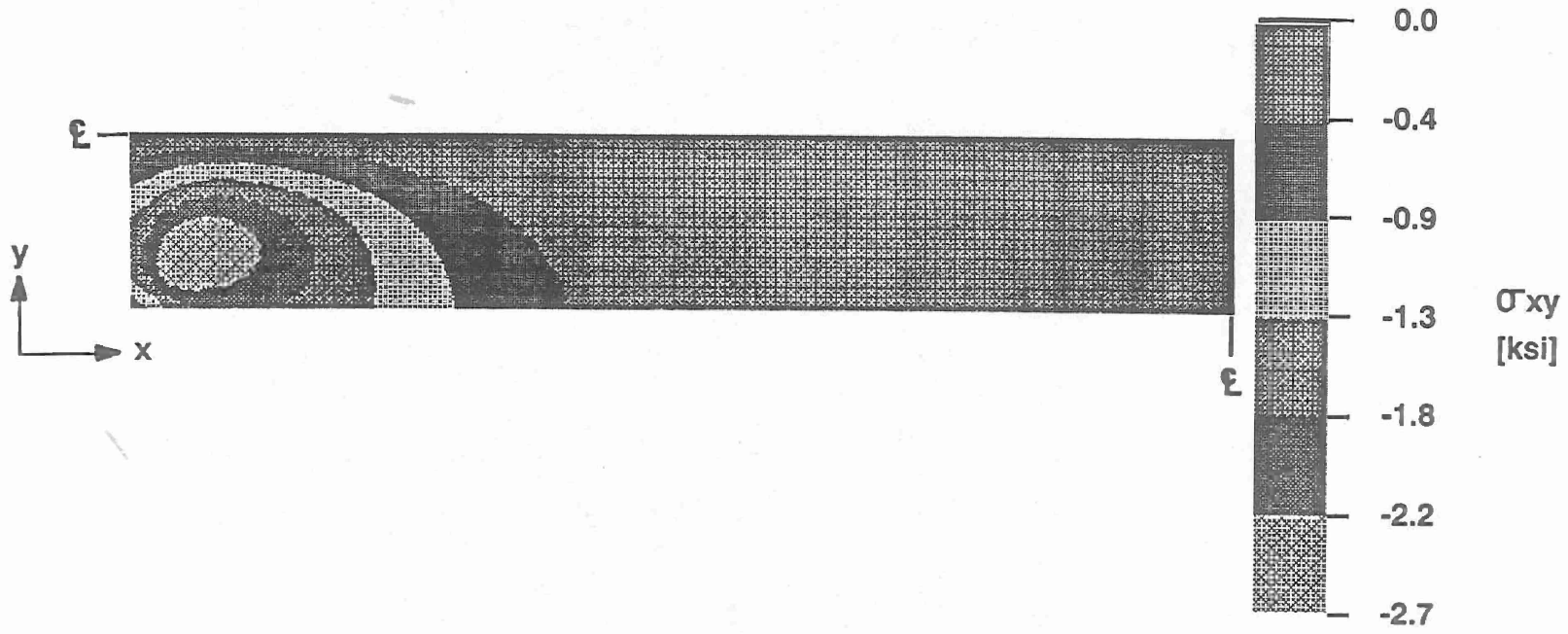

Figure 9: Rectangular Composite Membrane - σxy Results at 25 PSI

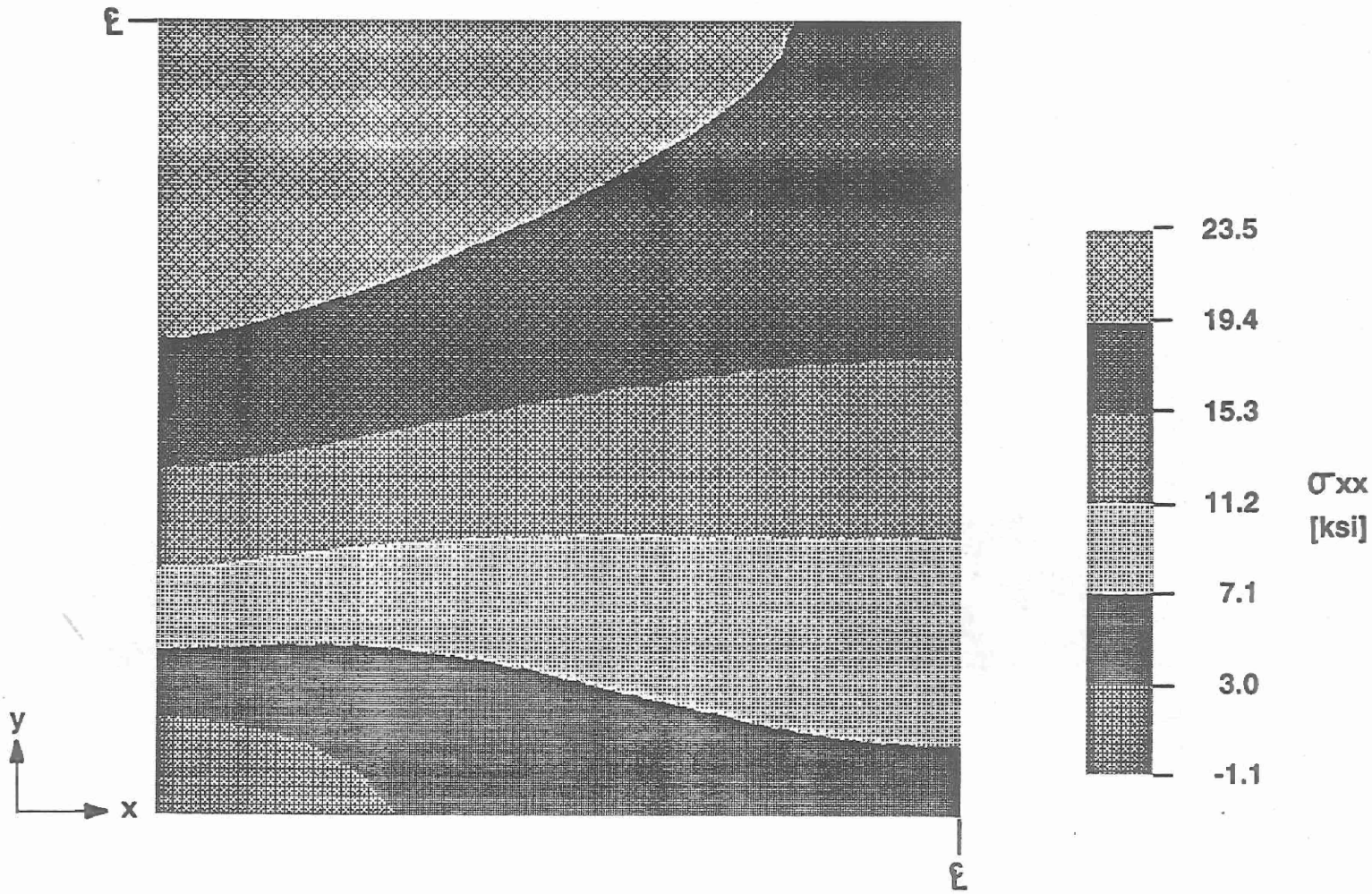

Figure 10: Square Composite Membranes - σxx Results at 25 PSI

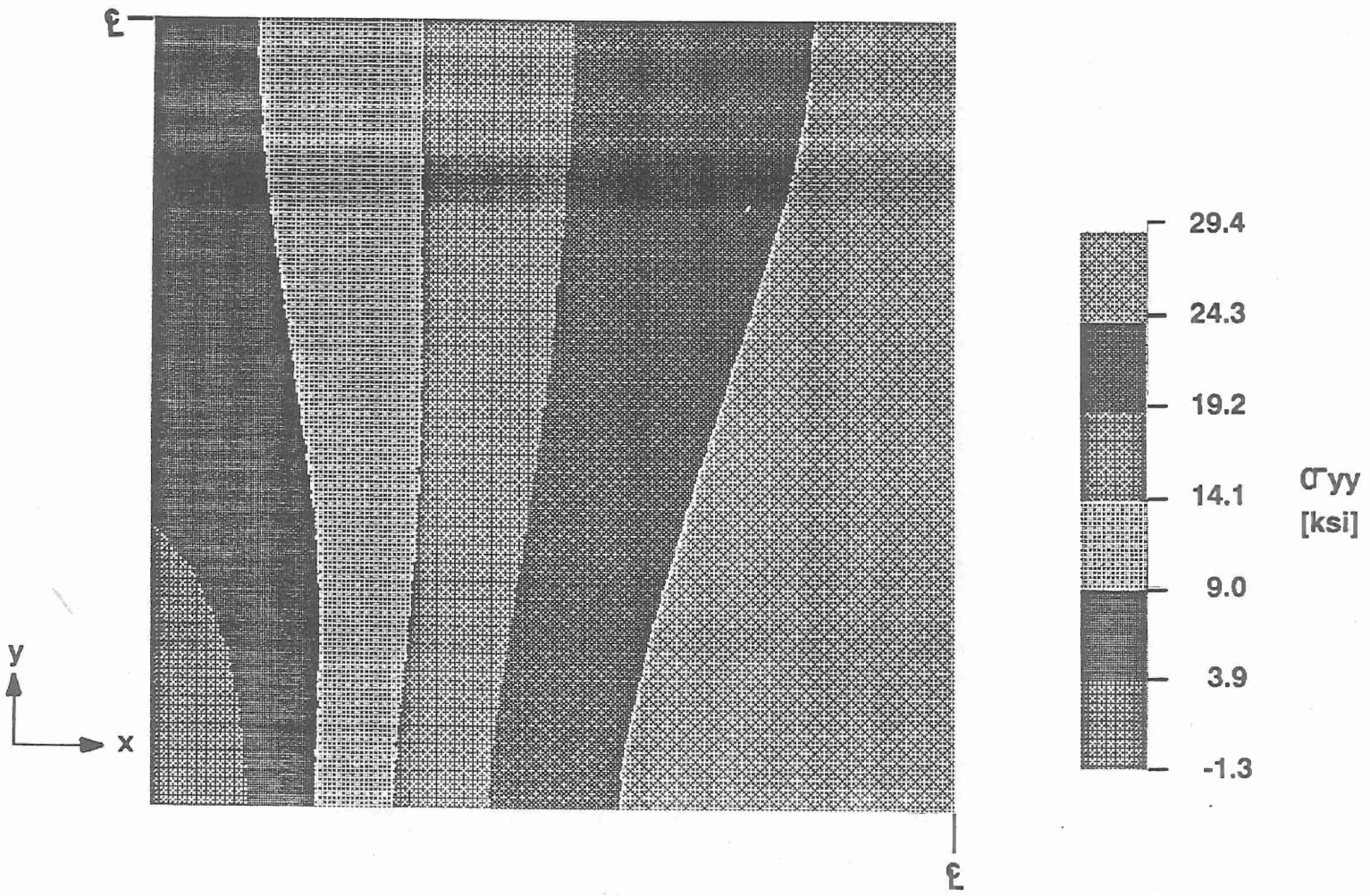

Figure 11: Composite Membrane - σyy Results at 25 PSI

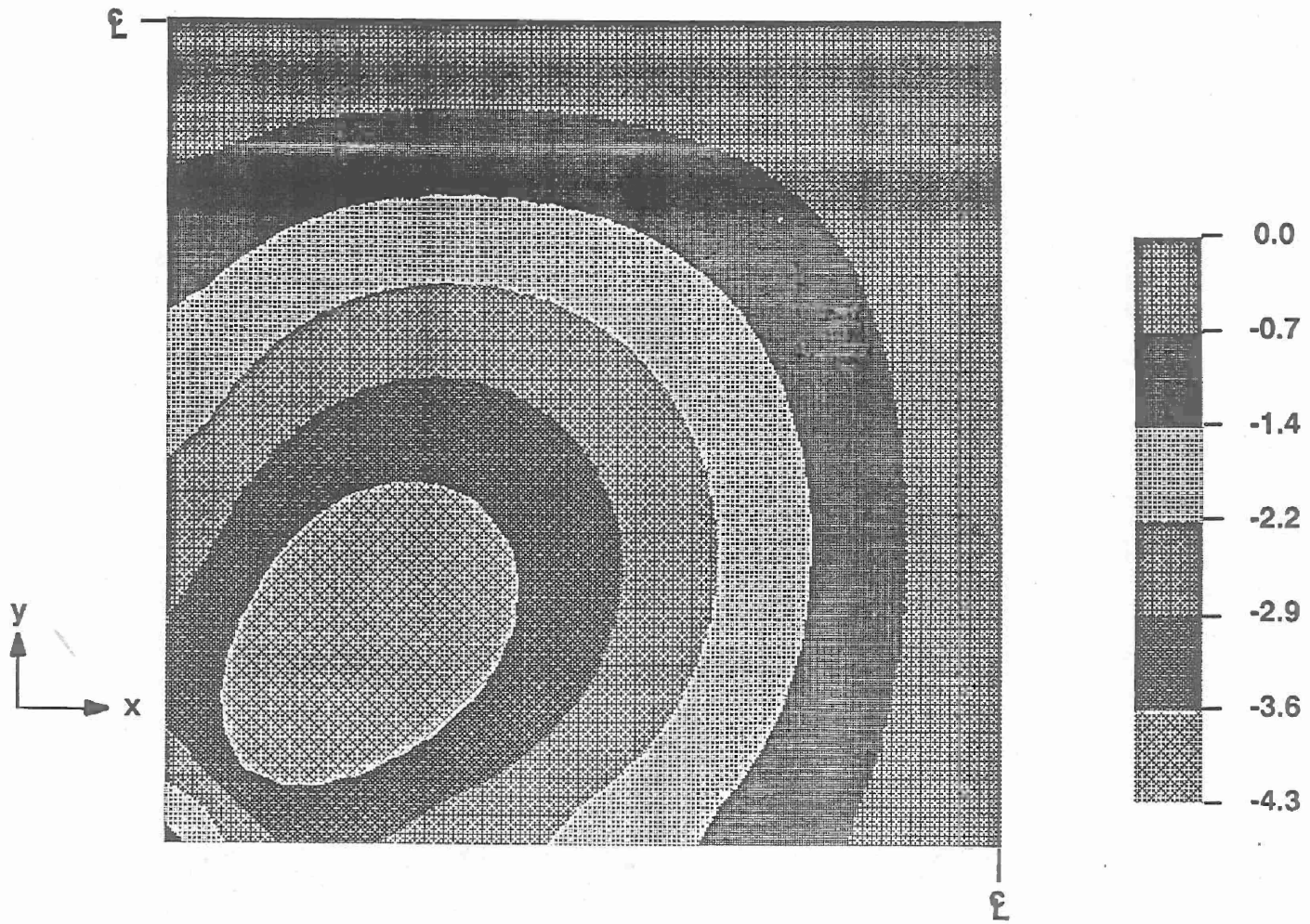

Figure 12: Composite Membrane - σxy Results at 25 PSI

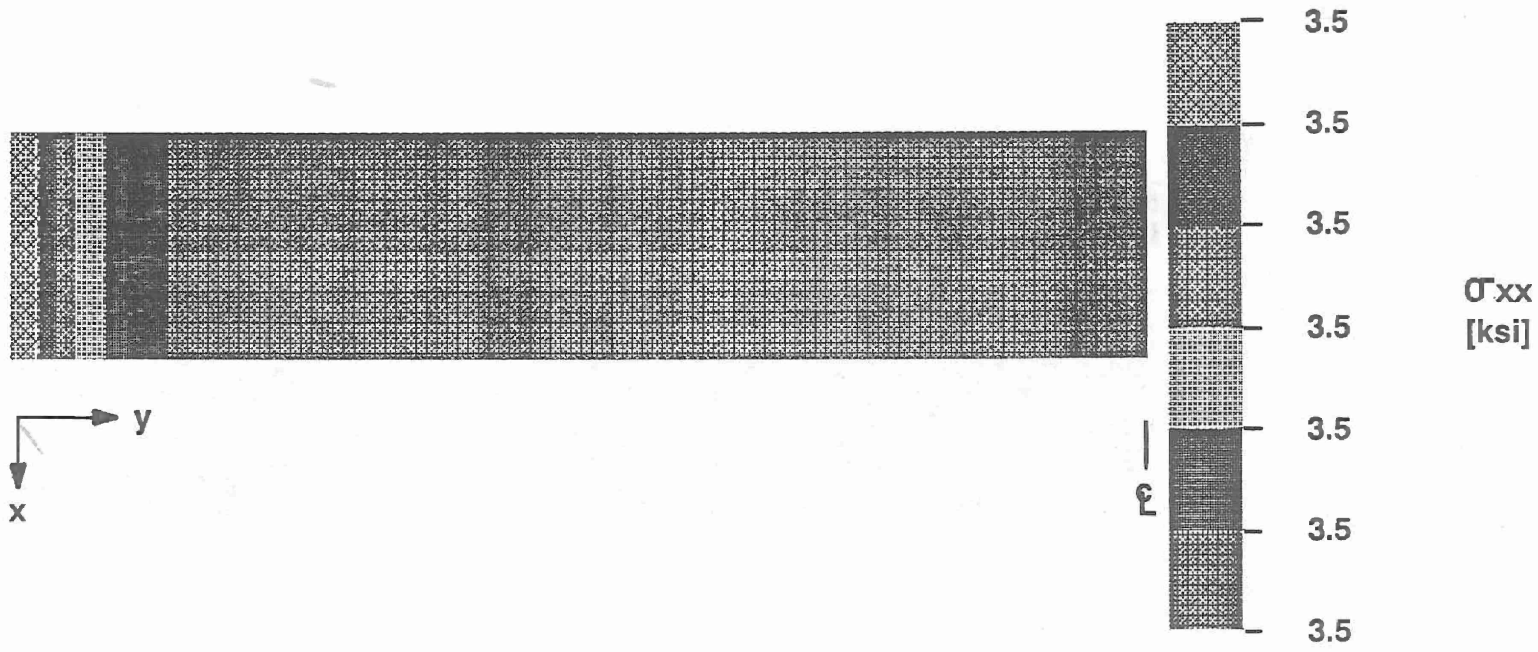

Figure 13: Infinite Composite Membrane - σxx Results at 25 PSI

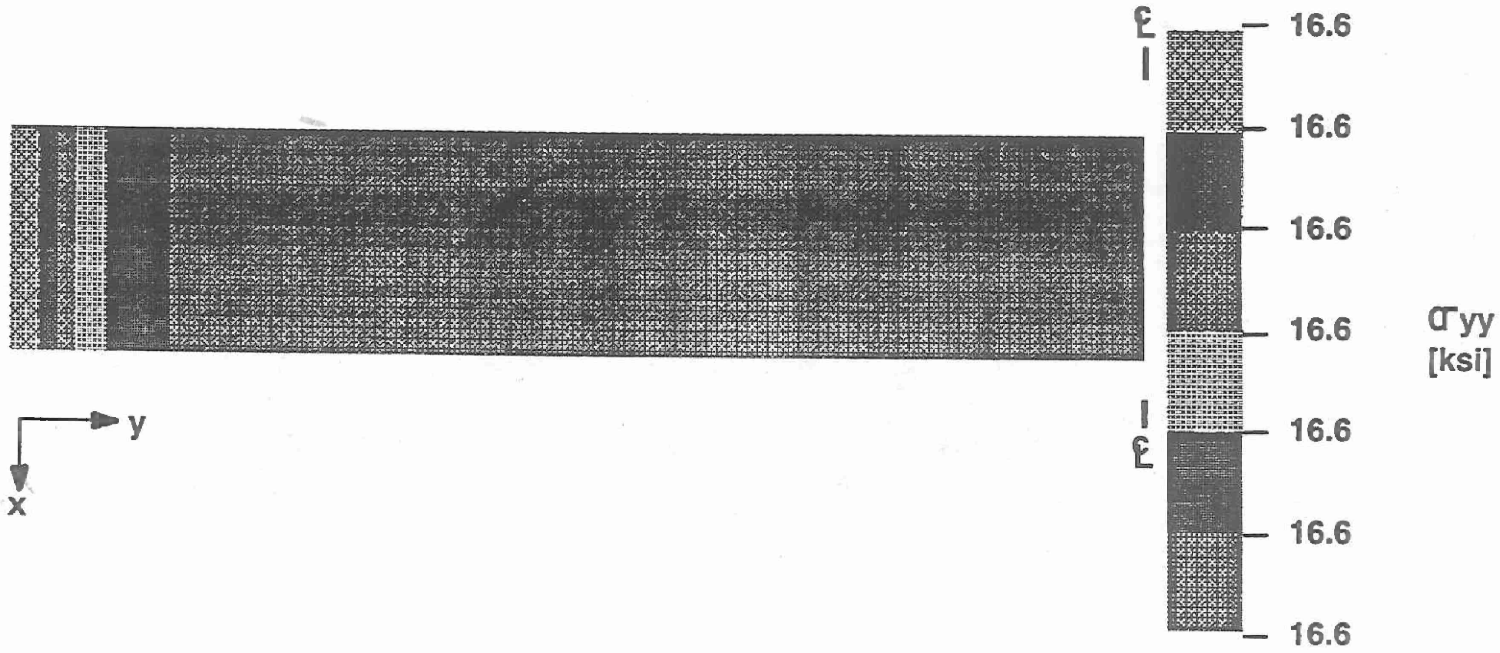

Figure 14: Infinite Composite Membrane - σyy Results at 25 PSI

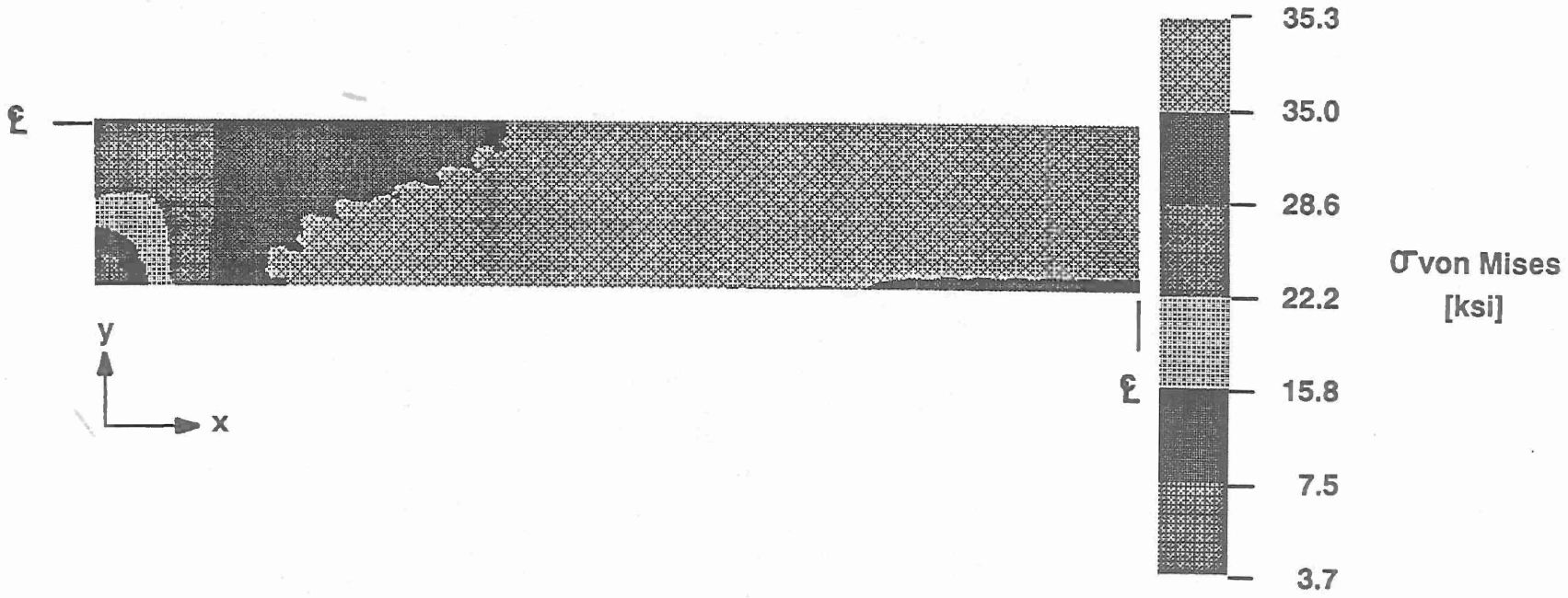

Figure 15: Rectangular Aluminum Membrane - Von Mises Stress Results
(One Load Increment After Onset of Yielding)

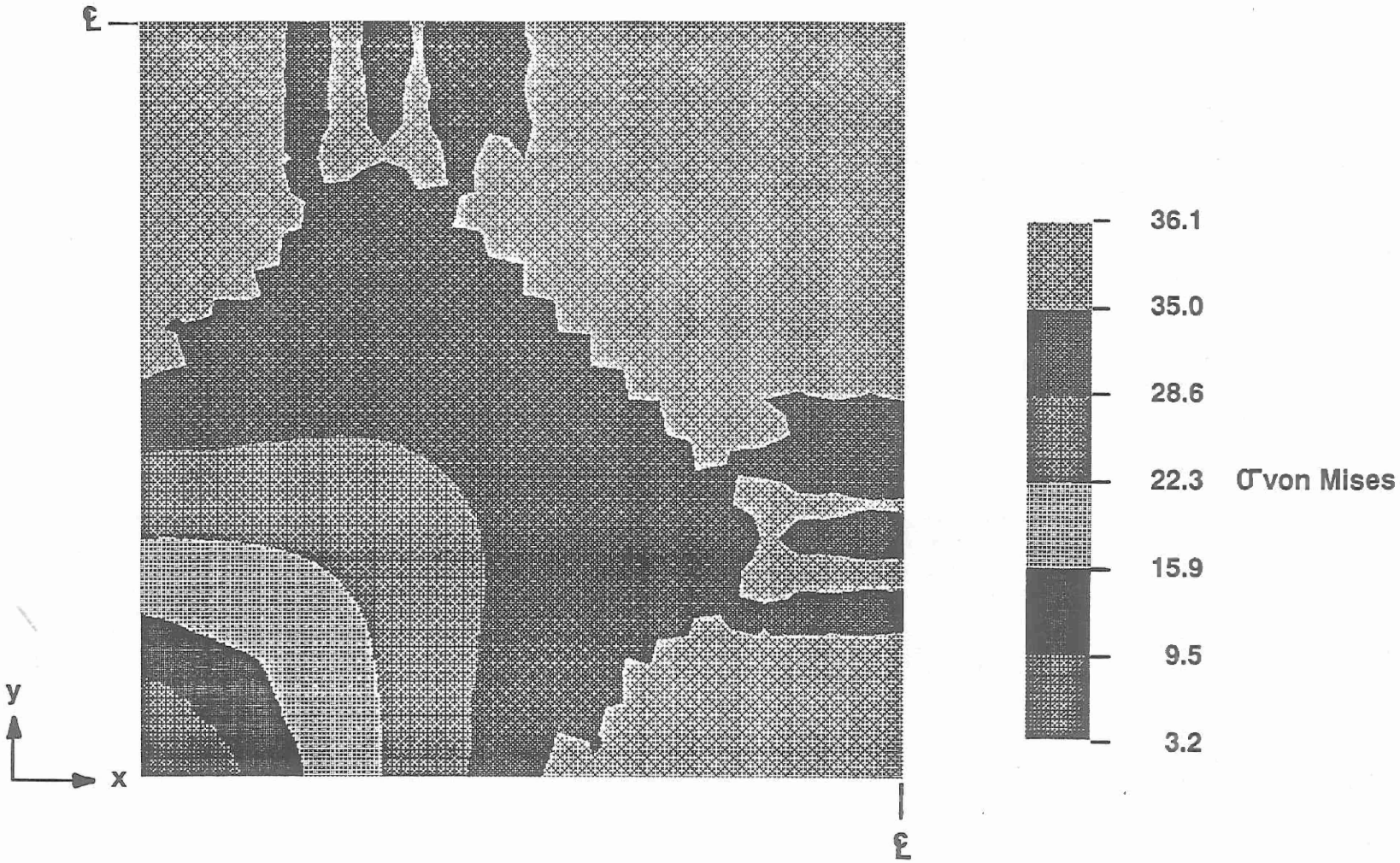

Figure 16: Square Aluminum Membrane - Von Mises Stress Results
(One Load Increment After Onset of Yielding)

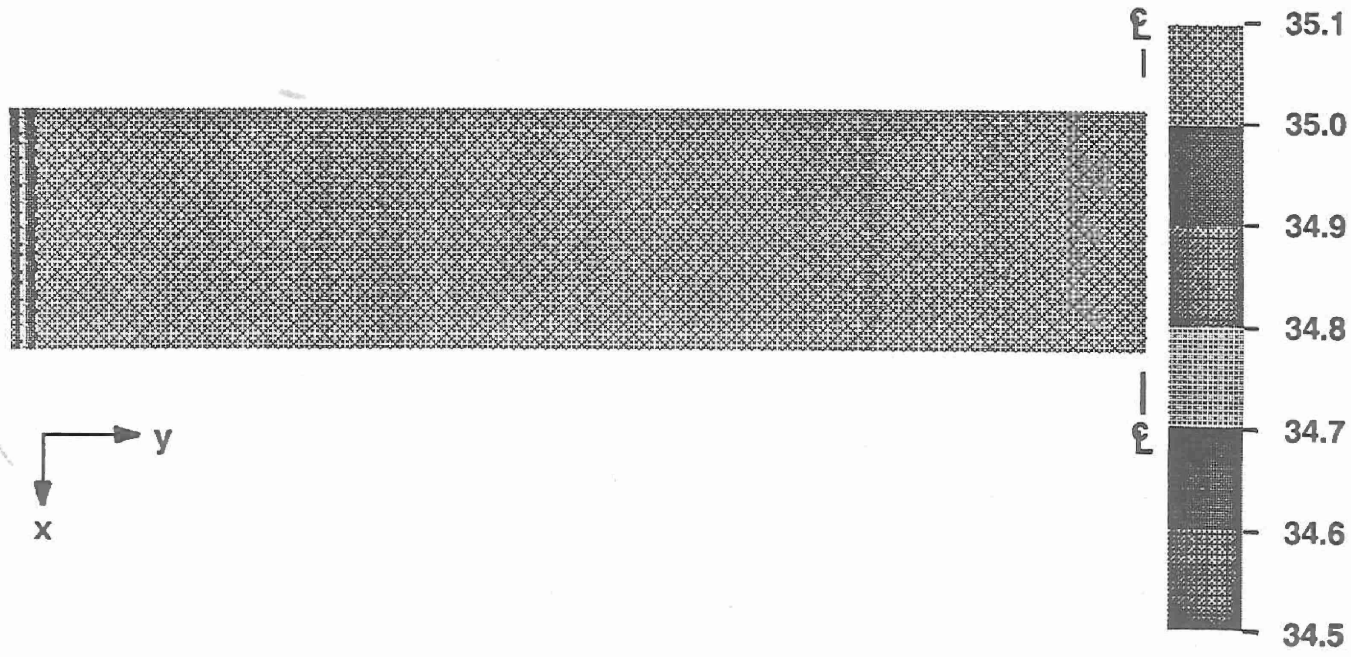

Figure 17: Infinite Aluminum Membrane - Von Mises Stress Results
(One Load Increment After Onset of Yielding)

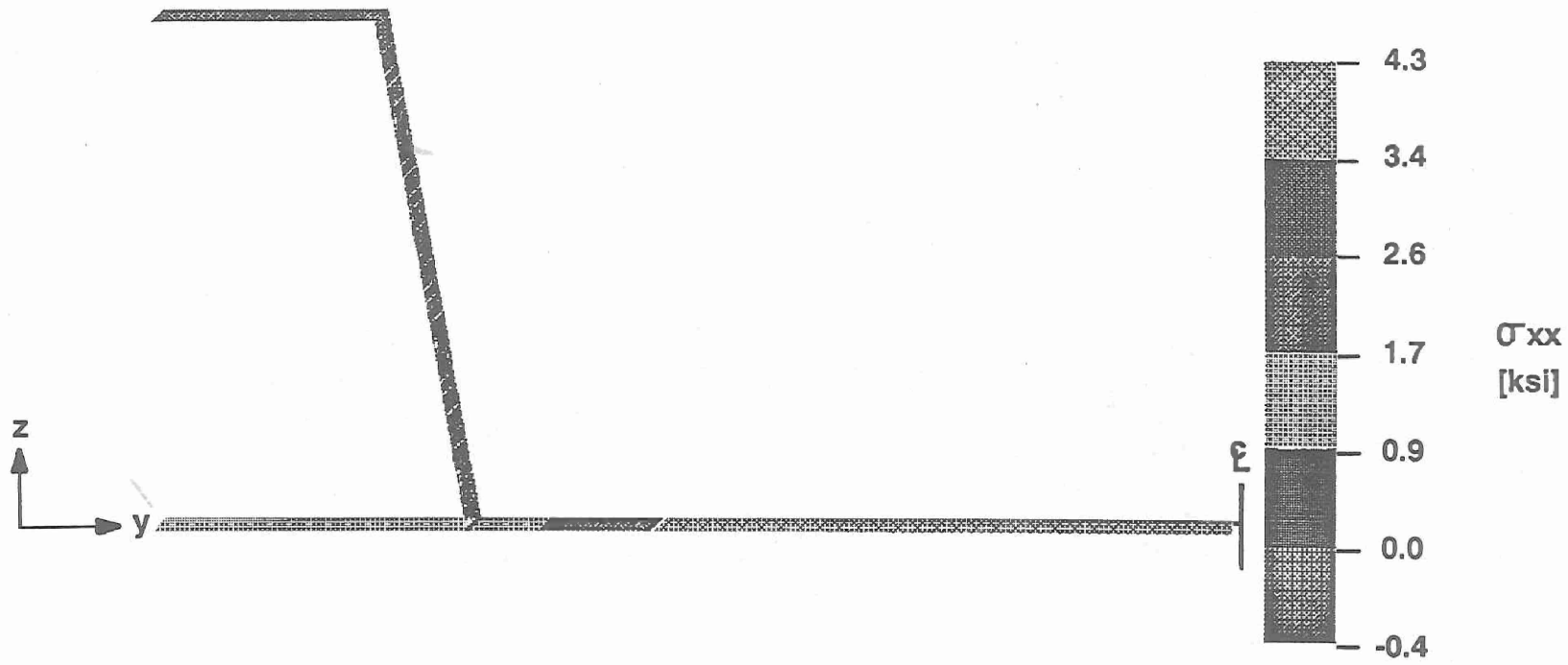

Figure 18: Infinite Composite Membrane with Stiffener
σxx Results at 25 PSI

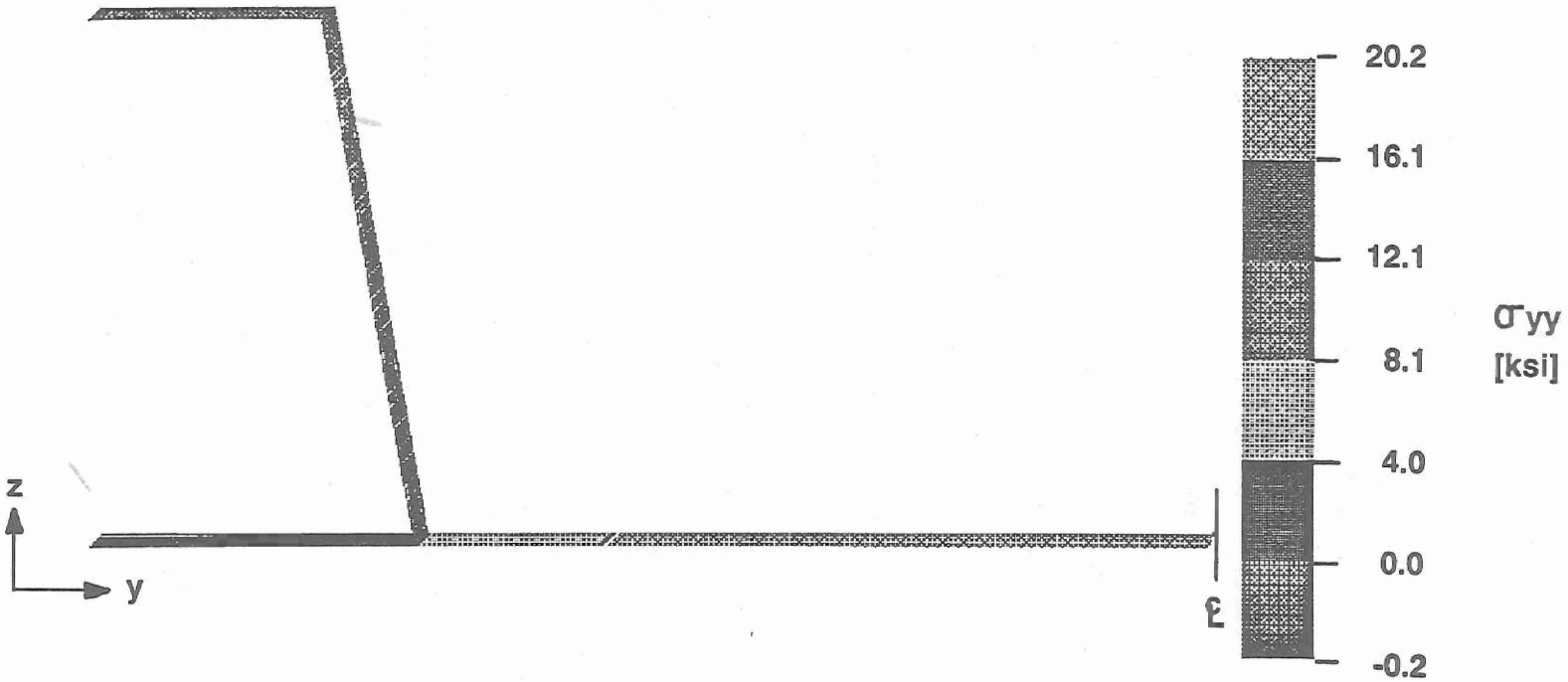

Figure 19: Infinite Composite Membrane with Stiffener
σyy Results at 25 PSI

laminate and the Tsai-Wu criterion was applied again to determine the ultimate failure safety factor. In the laminates with only fabric plies, any ply failure resulted in the loss of strength and stiffness of half the plies. In all such cases, the remaining plies were immediately overloaded. Ultimate failure was then triggered and two safety factors are therefore equivalent for these laminates.

The safety factors are listed in Table 4. The critical points for failure of the rectangular membranes were found to be at the boundaries near the ends rather than the membrane center. The ply failures of the 90° plies occurred at the midpoint of the short edge of the specimen. Most of the ultimate failures occurred along the long edge, although relatively close to the end. The critical point for the square membranes was found to be the midpoint of the sides. The infinitely long membranes were found to have a nearly constant stress state across the entire width, indicating failure in an actual structure could initiate anywhere along the span.

Discussion

For thin rectangular pressure-loaded plates, linear plate theory begins to give way to cubic membrane behavior when maximum deflection is on the order of the plate thickness. The behavior remains cubic as long as the material remains linearly elastic.

The aluminum membranes experienced a significant decrease in tangent modulus after yielding which resulted in load-deflection behavior approaching linearity. This linearity can be understood by examining the extreme case of elastic-perfectly plastic behavior. Once the behavior is perfectly plastic, the stress level is independent of deflection. Geometrically altering the angular deflection at the boundary (and therefore the out-of-plane force component) becomes the only means for increasing the reaction force when the pressure load is increased. If the deflection "mode shape" is relatively constant with small out-of-plane angular deflection at the boundaries, then the "amplitude" (and therefore the center deflection and the out-of-plane force component) must be proportional to the load level.

The ultimate strength safety factors imply that composite fabric plies with the fibers oriented in the principal directions of the membrane (i.e., the $[0/90]_s$ laminate) are the most efficient. These laminates have the highest safety factors and will not fail if subjected to the dynamic impact of a 10 psi pressure wave. Since the equivalent maximum pressure level for a 10 psi pressure wave is 101.2 psi and the pressure level analyzed 25 psi, the safety factor necessary to assure structural survival is the ⅔ power of their ratio, or 2.54.

The inclusion of 90° unidirectional plies is detrimental because of their inherent weakness in the laminate's longitudinal

Table 4: Safety Factors for Glass/Epoxy Membranes at a Pressure of 25 psi

Lamination Sequence	Infinite Membrane		Rectangular Membrane		Square Membrane		Infinite Membrane with Stiffener	
	FPF[a]	Ult[b]	FPF	Ult	FPF	Ult	FPF	Ult
$[0_f/90_f]_s$	3.12	3.12	2.80	2.80	1.89	1.89	1.92	1.92
$[0_f/90_f/\overline{90}_t]_s$	1.86	3.47	0.46	3.03	0.20	1.61	1.54	2.86
$[\pm 9.1_f]_s$	—	—	1.94	1.94	—	—	—	—
$[\pm 9.1_f/\overline{90}_t]_s$	—	—	0.45	2.79	—	—	—	—
$[\pm 35.9_f]_s$	—	—	2.14	2.14	—	—	—	—
$[\pm 35.9_f/\overline{90}_t]_s$	—	—	0.37	2.42	—	—	—	—
$[\pm 45_f]_s$	2.23	2.23	2.13	2.13	1.30	1.30	1.37	1.37
$[\pm 45_f/\overline{90}_t]_s$	1.73	2.65	0.36	2.24	0.18	1.10	1.43	2.18

[a] First Ply Failure
[b] Ultimate

direction. Splits along the fiber direction require shear transfer through neighboring plies. The resulting stress concentrations can weaken the entire laminate. If first ply failure is acceptable and the assumptions regarding post-first ply failure are adequate, then laminates with 90° unidirectional plies have a slight strength advantage because the 90° unidirectional plies, even when damaged, reduce the maximum deflection and therefore stress level in the fabric plies. Although fabric plies in general may suffer some internal damage before overall ply failure, the fibers remain largely intact and the plies retain most of their strength and stiffness without relying on shear transfer through neighboring plies. Thus, the laminates containing all fabric plies are superior if first ply failure is to be avoided.

Results suggest that high aspect ratio membranes are more weight efficient for membranes of given area. As the aspect ratio of the membrane is reduced, the width of the membrane must be increased to preserve area. Wider membranes at the same pressure level will have greater deflection and will have to react far greater out-of-plane load per unit length of the boundary. Thus, either the pressure level must be reduced or the membrane thickness must be increased to maintain the same ultimate failure safety factor.

When determining ultimate strengths, the critical location is the end region where the deflection field transitions from the far field distribution to the end boundary conditions. The infinite membrane analysis gives excellent agreement with the full model for stress and deflection distributions away from the ends. Nonetheless, the model which includes the end region is needed for sufficient strength characterization. It can also be noted that the infinite model has a nearly constant stress field across the membrane width. This is analogous to a section of an infinitely long balloon inflated to form a right circular cylinder.

The results of the bilinear aluminum models indicate that these membranes do not approach their ultimate strain at 25 psi. The aluminum membrane behavior is rather complex because the load-deflection behavior reverts from cubic to linear after yielding. Permanent deformations can accumulate after each oscillation resulting in further complications. Since the failure of biaxially loaded metals after yielding and permanent deformation is not well understood, it is not possible to conclude from this analysis whether or not a particular aluminum membrane configuration would survive a particular loading. Metal membranes should be tested experimentally, possibly via shock tube tests. If an aluminum membrane can provide the same protection against pressure loading as a composite membrane with a similar areal density, its advantages in manufacturing and electromagnetic shielding would make it an attractive alternative.

Stiffeners significantly affect the global behavior of infinite strip membrane models. The absolute center deflection and the applied pressure no longer have a cubic relationship. This

results from the displacement of the membrane boundaries. The out-of-plane displacement of the boundaries adds to the overall deflection. The transverse displacement tends to stretch the membrane tighter. The effects of the stiffener interact in a complex manner, even to the point of decreasing the center deflection of the aluminum membrane. This results in part from the side forces from the applied pressure on the stiffener webs. The effects of the stiffener behavior could be more pronounced in models allowing for the length dimension of the membrane and bending of the stiffener. The dynamic behavior of the entire structure then involves complex interactions between linear and nonlinear components.

Conclusions

The results of the analyses in this investigation support the following conclusions:

1. The load-deflection behavior of a thin materially linear membrane is cubic once the deflection is greater than the order of the membrane thickness. After yielding and its related significant reduction in tangent modulus, the load-deflection behavior of bilinear aluminum membranes approaches linearity.

2. The most effective lamination sequences for square or rectangular composite membranes appear to be fabric plies with the fibers oriented along the major axes of the membrane.

3. The most effective configuration for rectangular membranes appears to be a long thin (high aspect ratio) membrane.

4. The most critical area for material failure of rectangular membranes is near the membrane's end. Thus, two-dimensional analyses which ignore end effects may be inadequate to properly predict membrane strength.

5. Aluminum membranes exhibit promise for providing protection from both pressure loading and electromagnetic interference. Nonetheless, the uncertainties regarding dynamic behavior and biaxial failure after yielding and permanent deformation will most likely require experimental study.

6. The use of membrane boundaries with finite stiffness (i.e. stiffeners) significantly affects global behavior of the membrane. Further analyses are warranted to investigate this behavior.

References

1. Timoshenko, S., and Woinowsky-Kreiger, S., Theory of Plates and Shells, McGraw-Hill, 1959, pp. 6-12.

2. Pagano, N. J., "Exact Solutions for Composite Laminates in Cylindrical Bending," *J. Composite Materials*, Vol. 3 (1969), pp. 398-411.

3. Shaw, F. S., and Perrone, N., "A Numerical Solution for the Nonlinear Deflection of Membranes," *J. Applied Mechanics*, Vol. 21, No. 2, June 1954, pp. 117-128.

4. Flügge, W., Handbook of Engineering Mechanics, McGraw-Hill, 1962, Section 45.14.

5. Remington, P. J., O'Callahan, J. C., and Madden, R., Analysis of Stresses and Deflections in Frame Supported Tents, Technical Report 75-31, US Army Natick Laboratories, April 1974, pp. 106-110.

6. Godfrey, T. A., Verification of Dynamic Load Factor for Analysis of Airblast Loaded Membrane Shelter Panels by Static and Dynamic Nonlinear Finite Element Calculations, Technical Note, US Army Natick Research, Development, and Engineering Center, 1991.

APPENDIX

Consider a mass m on a nonlinear spring on which the magnitude of the restoring force is proportional to the cube of the displacement x:

$$F_{spring} = kx^3 \tag{A.1}$$

At time t = 0, an external force F_0 is applied as a step function in the positive x direction. The equation of motion can thus be written:

$$F_0 - kx^3 = m\ddot{x} \tag{A.2}$$

The equilibrium displacement for the static case, x_s, can be determined directly from Equation A.1:

$$F_0 = kx_s^3 \tag{A.3}$$

Substituting A.3 into A.2 and rearranging the terms yields:

$$m\ddot{x} + k(x^3 - x_s^3) = 0 \tag{A.4}$$

Displacements can be nondimensionalized by the static value:

$$\chi = \frac{x}{x_s} \tag{A.5}$$

and a convenient constant A can be defined:
Equation A.4 can now be written:

$$A\ddot{\chi} + \chi^3 - 1 = 0 \tag{A.6}$$

$$A = \frac{m}{kx_s^2} \tag{A.7}$$

If both sides of the equation are multiplied by the derivative of χ with respect to time, it becomes:

$$A\ddot{\chi}\dot{\chi} + \chi^3\dot{\chi} - \dot{\chi} = 0 \tag{A.8}$$

Equation A.8 can be rewritten as:

$$\frac{d}{dt}\left(\frac{A}{2}\dot{\chi}^2 + \frac{1}{4}\chi^4 - \chi\right) = 0 \tag{A.9}$$

This implies:

$$\frac{A}{2}\dot{\chi}^2 + \frac{1}{4}\chi^4 - \chi = C \qquad (A.10)$$

where C is a constant. The initial conditions are such that:

$$\dot{\chi}(0) = \chi(0) = 0 \qquad (A.11)$$

Thus, C is identically zero:

$$\frac{A}{2}\dot{\chi}^2 + \frac{1}{4}\chi^4 - \chi = 0 \qquad (A.12)$$

At the extremum values of χ, its derivative with respect to time will be zero. Thus, the maximum and minimum values of χ satisfy the following equation:

$$\frac{1}{4}\chi^4 - \chi = 0 \qquad (A.13)$$

It can be seen by inspection that χ_{max} and χ_{min} are given by:

$$\chi_{max} = \sqrt[3]{4} \quad ; \quad \chi_{min} = 0 \qquad (A.14)$$

The implication of this result on the analysis in the text is that the static pressure that must be applied to achieve the same deflection and stress state experienced at the maximum deflection is four times the actual dynamically applied pressure.

This document reports research undertaken at the US Army Natick Research, Development and Engineering Center and has been assigned No. NATICK/TR-92/018 in the series of reports approved for publication.